Rare Metal Materials and Engineering
Volume 49, Issue 12, December 2020
Available online at www.rmme.ac.cn

Science Press

Cite this article as: Rare Metal Materials and Engineering, 2020, 49(12): 4129-4141.

ARTICLE

Six Different Mathematical Models to Predict the Hot Deformation Behavior of C71500 Cupronickel Alloy

Gao Xin[1,2,3], Wu Huibin[4], Tang Di[1], Li Defu[2], Liu Ming[5], Zhou Xiangdong[3]

[1] Institute of Engineering Technology, University of Science and Technology Beijing, Beijing 100083, China; [2] General Research Institute of Nonferrous Metals, Beijing 100088, China; [3] Wuxi Longda Metal Material Co., Ltd, Wuxi 214105, China; [4] Collaborative Innovation Center of Steel Technology, University of Science and Technology Beijing, Beijing 100083, China; [5] State Key Laboratory for Strength and Vibration of Mechanical Structures, Xi'an Jiaotong University, Xi'an 710049, China

Abstract: Base on the Gleeble-3500 thermo mechanical simulator, the real stress-strain data of C71500 cupronickel alloy in isothermal compression test were obtained in the temperature range of 1073~1273 K and strain rate range of 0.01~10 s^{-1}. Johnson-Cook, modified Johnson-Cook, modified Zerilli-Armstrong, Arrhenius-type, Fields-Backofen-Zhang and Zhou-Guan models were used to regress the constitutive equation of high temperature flow stress. The applicability of the six models was evaluated by comparing the accuracy, correlation coefficient (R), root mean square error (RMSE), average absolute relative error (AARE), the number of uncertainty and the time consuming for calculation of these parameters. According to the fitting results of parameters and time consumption, the Zhou-Guan model is the best for predicting the deformation resistance of C71500 alloy at different strain rates and temperatures. The most suitable thermal deformation constitutive equation of C71500 alloy is established, which will provide the basic data for the design of the hot working process and the simulation analysis of the thermal deformation process of the alloy. In addition, this research can provide important reference in the same field.

Key words: Cu/Al bimetal; interfacial microstructure; intermetallic compounds; shear strength

Cupronickel alloys (primarily C70600, C71000 and C71500) are commonly utilized as the engineering materials for the manufacture of ship condensing pipes[1], the heat exchanger of coastal power plant, the pipes of desalination plant, the hull and some marine engineering applications, because of their good corrosion resistance[2-10], fine mechanical working ability[11,12], good ductility, excellent conductivity and thermal conductivity, and excellent antifouling performance in the sea water. According to the statistics, the consumption of cupronickel alloy in merchant and military ships accounts for 2%~3% of the total mass[13].

In the process of the hot deformation, the constitutive equation of materials is complex, and the hardening and softening processes of alloys are significantly affected by strain rate, strain and distortion temperature[14]. Thus, a fully understanding of the flow behavior of the material is strongly necessary for designing the processes of hot working[15]. The description of rheological process only uses a few parameters by empirical and semi-empirical models, which are widely used to predict the thermal deformation behavior of metal materials. These models include Johnson-Cook[16], modified Johnson-Cook[17], modified Zerilli-Armstrong[18,19], Arrhenius-type[20-22], Fields-Backofen[23-26], Fields-Backofen-Zhang[27], Zhou-Guan[28], and Khan-Huang-Liang[29] models, etc. Since the validation of these models are based on the steel[30,31], titanium[32], aluminum[33] and magnesium alloys[34], the applicability of cupronickel alloy needs to be verified. Although some scholars[35,36] have analyzed the constitutive model of cupronickel alloy, they all adopted just a single model.

In this research, six common models are used to analyze the

Received date: May 13, 2020
Foundation item: National Strong Foundation Project of China (TC170A2KN-8); Industrialization Project of Scientific and Technological Achievements in Wuxi City (CYE22C1706); Wuxi Enterprise Academician Workstation (BM2018503); National Natural Science Foundation of China (51801149)
Corresponding author: Wu Huibin, Ph. D., Professor, Collaborative Innovation Center of Steel Technology, University of Science and Technology Beijing, Beijing 100083, P. R. China, Tel: 0086-10-62332598, E-mail: whbustb@163.com

deformation resistance of C71500 cupronickel alloy, and the correlation coefficient (R), root mean square error (RMSE) and average absolute relative error (AARE) are employed to verify the practicability of the models and to find out the most suitable one for cupronickel alloy. With the complexity of the section shape and the improvement of processing speed, the tonnage of thermal processing equipment for cupronickel alloy increased. The accuracy of rheological stress model can provide a theoretical basis for the selection and verification of thermal deformation equipment.

1 Experiment

The material used in this study was C71500 cupronickel alloy with lower C, O and S element content. The chemical composition was: 30.54wt% Ni, 0.93wt% Mn, 0.80wt% Fe and balance Cu. The compression test was carried out using a cylindrical specimen with the height of 15 mm and diameter of 10 mm. The isothermal hot compression test was carried out on a Gleeble-3500 thermo-simulation system. The test temperature range was 1023~1273 K, the interval was 50 K and the true strain rate was 0.01, 0.1, 1 and 10 s^{-1}. The reduction in height was 50% of the original by the end of the compression tests. The detailed experimental procedure is shown in Fig.1. Each specimen was heated to 1323 K at a rate of 10 K/s, held for 3 min to make the sample uniformly heated, and then cooled at a rate of 5 K/s to reach the isothermal conditions for 30 s before compression tests. The true stress-strain curve obtained from the test is shown in Fig.2. The deformation resistance of C71500 alloy decreases with the increase of temperature and deformation rate, which conforms to the law of dynamic recovery and recrystallization of metal materials. However, the dynamic recrystallization of the material is very small, which shows that the stress does not decrease obviously with the increase of the strain, so it is more significant to choose an appropriate constitutive equation.

2 Results

2.1 J-C model

The Johnson-Cook (J-C) model can be indicated as follows[16]:

$$\sigma=(A+B\varepsilon^{n})(1+C\ln\dot{\varepsilon})(1-T^{*m}) \quad (1)$$

where σ, ε, A, B, and n are the equivalent flow stress (MPa),

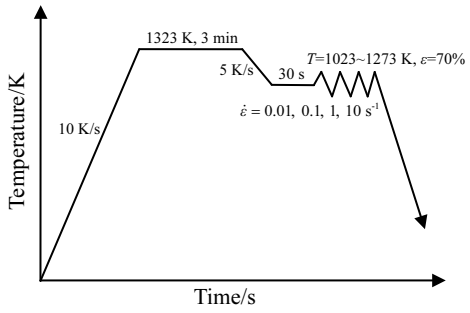

Fig.1 Experimental procedure of hot compression test for C71500 alloy

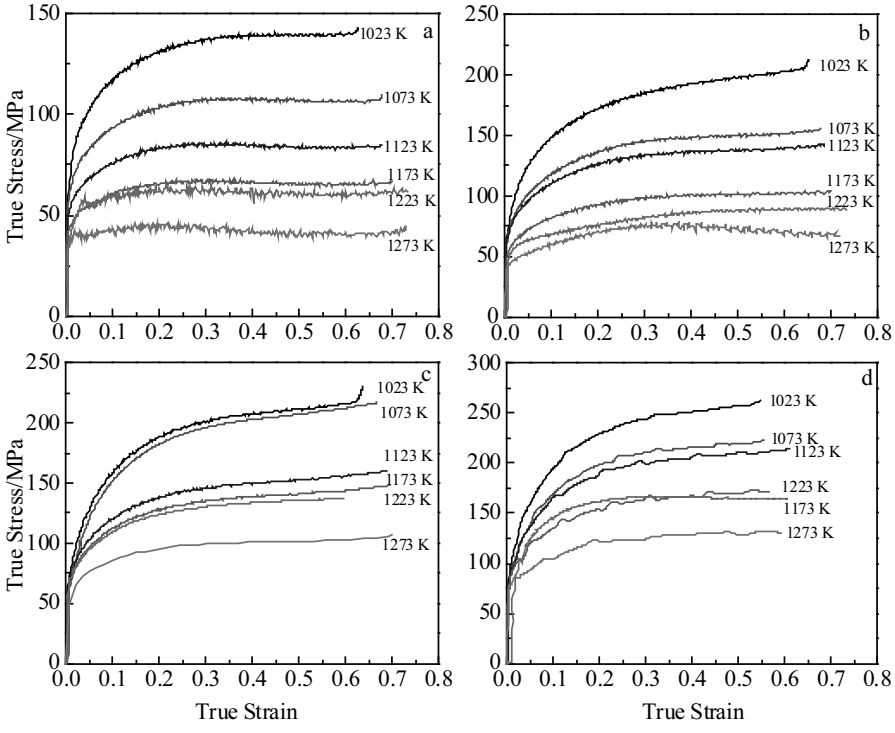

Fig.2 True stress-strain curves of C71500 alloy at different temperatures and strain rates: (a) 0.01 s^{-1}, (b) 0.1 s^{-1}, (c) 1 s^{-1}, and (d) 10 s^{-1}

plastic strain, yield stress, strain hardening coefficient, and strain hardening exponent, respectively; C and m are the strain hardening rate and thermal softening exponent coefficient, respectively; $\dot{\varepsilon}^* = \dot{\varepsilon}/\dot{\varepsilon}_0$ is the dimensionless strain rate ($\dot{\varepsilon}$ is the strain rate and $\dot{\varepsilon}_0$ is the reference strain rate); $T^*=(T-T_r)/(T_m-T_r)$, where T, T_m, and T_r are the absolute, melting and reference temperatures, respectively.

The temperature of 1023 K is taken as reference temperature (T_r) and the strain rate of 1 s^{-1} is assumed to be the reference strain rate ($\dot{\varepsilon}_0$) to acquire the material constants of the J-C model. A can be measured as 58.5926 MPa and T_m is 1468.7 K. The material constants of the J-C model can be easily evaluated by measuring stress-strain data.

2.1.1 Calculation of n and B

Eq.(1) can be expressed as follows at the reference temperature and reference strain rate:

$$\sigma = (A + B\varepsilon^n) \tag{2}$$

Take logarithm on both sides of Eq.(2):

$$\ln(\sigma - A) = \ln B + n\ln\varepsilon \tag{3}$$

By substituting the stress and strain values into Eq.(3), the relationship between $\ln(\sigma - A)$ and $\ln\varepsilon$ can be obtained, as shown in Fig.3. Through linear-regression analysis of the $\ln(\sigma - A)$ - $\ln\varepsilon$ plots, the values of n and B can be obtained as 0.236 57 and 183.4771 MPa, respectively.

2.1.2 Calculation of C

Eq.(1) can be expressed as follows when the deformation temperature is 1023 K and T^*=0 without flow softening term:

$$\frac{\sigma}{(A + B\varepsilon^n)} = 1 + C\ln\dot{\varepsilon}^* \tag{4}$$

By selecting series of strain (0.1~0.6), the relationship between $\sigma/(A+B\varepsilon^n)$ and $\ln\dot{\varepsilon}$ can be analyzed, as shown in Fig.4. The material constant C obtained by linear fitting method is 0.077 16. In Fig.4, only the average fitting line is shown.

2.1.3 Determination of m

At reference strain rate of Eq.(1),

$$\frac{\sigma}{(A + B\varepsilon^n)} = (1 - T^{*m}) \tag{5}$$

Take logarithm on both sides of Eq.(5):

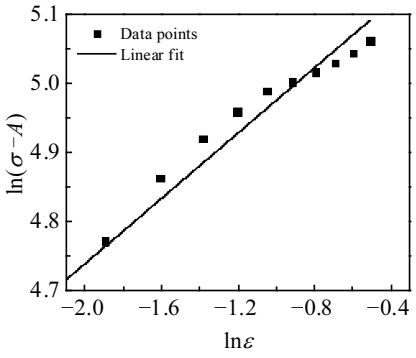

Fig.3 Relationship between $\ln(\sigma-A)$ and $\ln\varepsilon$

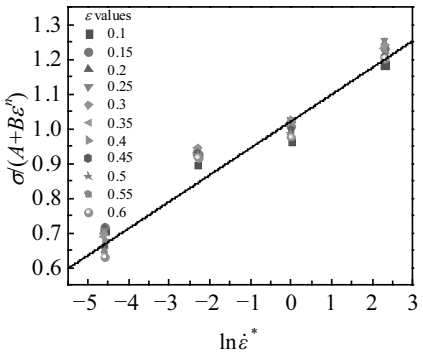

Fig.4 Relationship between $\sigma/(A+B\varepsilon^n)$ and $\ln\dot{\varepsilon}^*$

$$\ln\left[1 - \frac{\sigma}{(A + B\varepsilon^n)}\right] = m\ln T^* \tag{6}$$

The relationship between $\ln[1-\sigma/(A+B\varepsilon^n)]$ and $\ln T^*$ can be obtained by substituting four different deformation temperatures (1123, 1173, 1223 and 1273 K) and the corresponding flow stresses under different strains into Eq.(6), as shown in Fig.5. Thus, the material constant m can be gained as 0.6073 by linear fitting method.

The material constants based on the J-C model are listed in Table 1. Hence, the specific constitutive equation based on J-C model is as follows:

$$\sigma = (58.5926 + 183.4771\varepsilon^{0.236\ 57})(1 + 0.077\ 16\ln\dot{\varepsilon}) \times \left\{1 - [(T - 1023)/445.7]^{0.6073}\right\} \tag{7}$$

The comparison of flow stress-strain curves between measured and predicted data by the J-C model at different strain rates is shown in Fig.6.

2.2 M-J-C model

Considering the yield and strain hardening portion in the J-C model and the coupling effects of the temperature and strain rate on the flow behavior, the modified Johnson-Cook (M-J-C) model can be described as follows[17,37-40]:

$$\sigma=(A_1+B_1\varepsilon+B_2\varepsilon^2)(1+C_1\ln\dot{\varepsilon}^*)\exp[(\lambda_1+\lambda_2\ln\dot{\varepsilon})T^*] \tag{8}$$

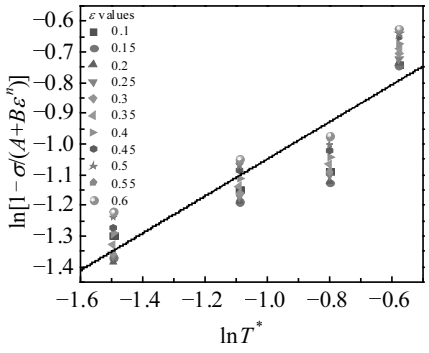

Fig.5 Relationship between $\ln[1-\sigma/(A+B\varepsilon^n)]$ and $\ln T^*$

Table 1 Parameters obtained by the J-C model

T_r/K	T_m/K	A/MPa	n	B	C	m
1023	1468.7	58.5926	0.236 57	183.4771	0.077 16	0.6073

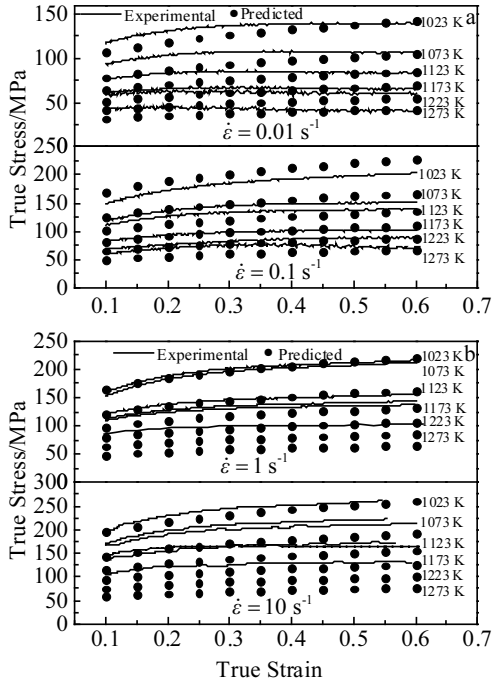

Fig.6 Comparison of flow stress between measured and predicted data by J-C model: (a) 0.01 s^{-1} and 0.1 s^{-1}; (b) 1 s^{-1} and 10 s^{-1}

The meaning of σ, ε, $\dot{\varepsilon}^*$, $\dot{\varepsilon}$, $\dot{\varepsilon}_0$, $T^*=T-T_r$, T and T_r are the same as that of the J-C model. A_1, B_1, B_2, C_1, λ_1, and λ_2 are the material constants.

Similarly, the same T_r and $\dot{\varepsilon}_0$ are used to evaluate the material constants of the M-J-C model.

2.2.1 Determination of A_1, B_1 and B_2

At reference temperature and strain rate ($T^*=0$, $\dot{\varepsilon}^*=1$), Eq.(8) can be expressed as follows:

$$\sigma=(A_1+B_1\varepsilon+B_2\varepsilon^2) \tag{9}$$

The relationship between σ and ε can be obtained by substituting the flow stress data obtained from the thermal compression test under different process conditions into Eq.(9), as shown in Fig.7. Then the values of A_1, B_1 and B_2 can be evaluated as 136.8453, 293.9874 and −279.723 MPa, respectively.

2.2.2 Determination of C_1

At reference temperature, Eq.(8) can be expressed as follows:

$$\frac{\sigma}{A_1+B_1\varepsilon+B_2\varepsilon^2}=(1+C_1\ln\dot{\varepsilon}^*) \tag{10}$$

The relationship between $\sigma/(A_1+B_1\varepsilon+B_2\varepsilon^2)$ and $\ln\dot{\varepsilon}^*$ can be obtained by substituting different strain rates and corresponding stresses into Eq.(10), as shown in Fig.8. Thus, the material constant C_1 can be obtained as 0.073 09 by linear fitting.

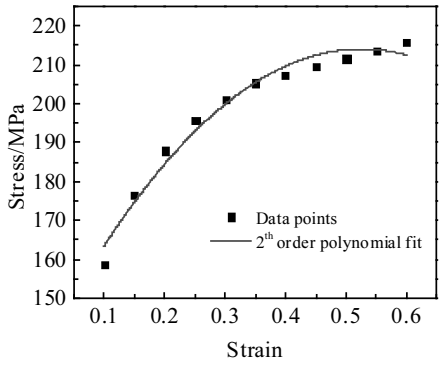

Fig.7 Relationship between σ and ε at the deformation temperature of 1023 K and strain rate of 1 s^{-1}

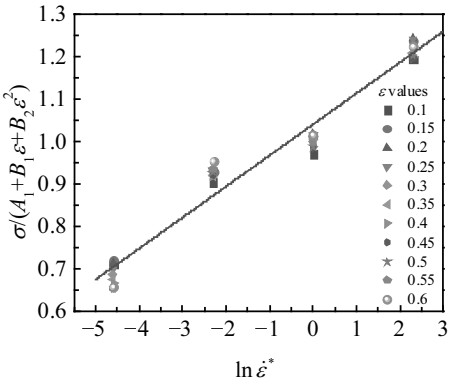

Fig.8 Relationship between $\sigma/(A_1+B_1\varepsilon+B_2\varepsilon^2)$ and $\ln\dot{\varepsilon}^*$

2.2.3 Determination of λ_1 and λ_2

A new parameter λ was introduced:

$$\lambda=\lambda_1+\lambda_2\ln\dot{\varepsilon}^* \tag{11}$$

The λ is a function of strain rate, i.e., Eq.(8) can be expressed as

$$\frac{\sigma}{(A_1+B_1\varepsilon+B_2\varepsilon^2)(1+C_1\ln\dot{\varepsilon}^*)}=e^{\lambda T^*} \tag{12}$$

Take the logarithm on both sides of Eq.(12),

$$\ln\left[\frac{\sigma}{(A_1+B_1\varepsilon+B_2\varepsilon^2)(1+C_1\ln\dot{\varepsilon}^*)}\right]=\lambda T^* \tag{13}$$

The relationship between $\ln[\sigma/(A_1+B_1\varepsilon+B_2\varepsilon^2)(1+C_1\ln\dot{\varepsilon}^*)]$ and T^* can be obtained at different strain rates, strain and deformation temperatures, as shown in Fig.9. Then, $\lambda_{(\dot{\varepsilon}^*=0.01)}$, $\lambda_{(\dot{\varepsilon}^*=0.1)}$, $\lambda_{(\dot{\varepsilon}^*=1)}$ and $\lambda_{(\dot{\varepsilon}^*=10)}$ is −0.004 37, −0.003 83, −0.002 74 and −0.002 43 when $\dot{\varepsilon}^*$ are 0.01, 0.1, 1 and 10, respectively (Fig.10).

According to Eq.(11), the values of λ_1 and λ_2 can be derived from the slope of the line $\lambda-\ln\dot{\varepsilon}^*$ as –0.003 and 0.000 300 097, respectively.

The material constants based on the M-J-C model for C71500

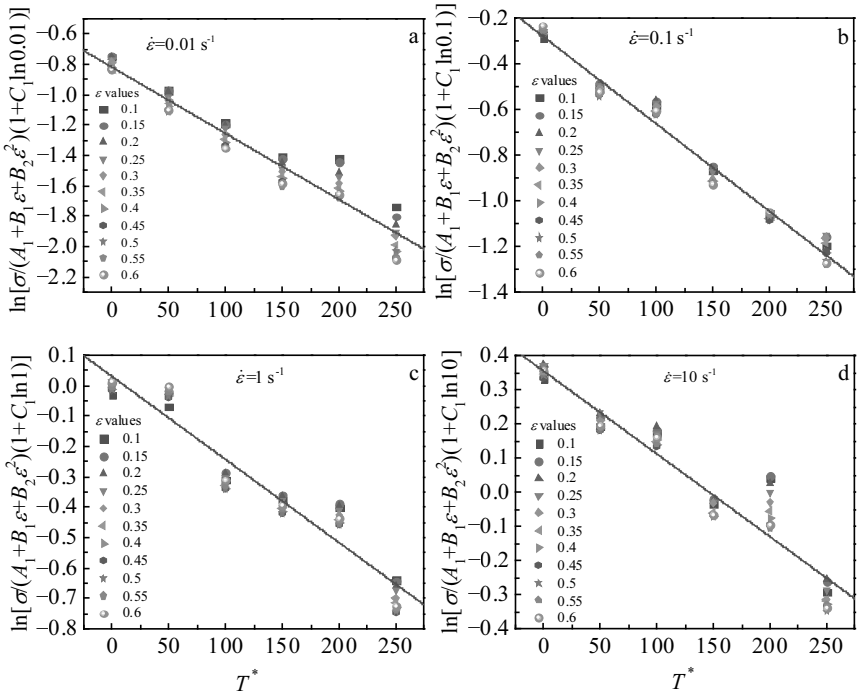

Fig.9 Relationship between $\ln[\sigma/(A_1+B_1\varepsilon+B_2\varepsilon^2)(1+C_1\ln\dot{\varepsilon}^*)]$ and T^* for different strain rates: (a) $\dot{\varepsilon}$=0.01 s^{-1}, (b) $\dot{\varepsilon}$=0.1 s^{-1}, (c) $\dot{\varepsilon}$=1 s^{-1}, and (d) $\dot{\varepsilon}$=10 s^{-1}

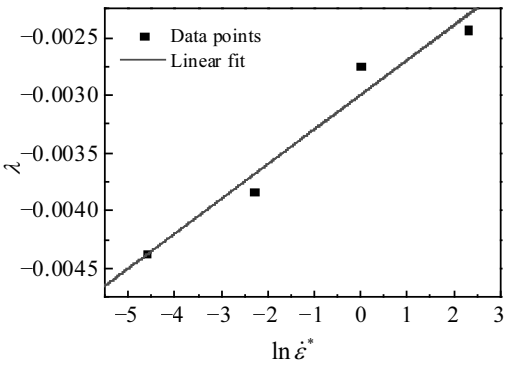

Fig.10 Relationship between λ and $\ln\dot{\varepsilon}^*$

alloy are given in Table 2. Finally, the specific constitutive equation based on M-J-C model can be obtained as follows:

$$\sigma=(136.845\ 28+293.9874\varepsilon-279.723\varepsilon^2)(1+0.073\ 09\ln\dot{\varepsilon}^*)\times \exp[(-0.003+0.000\ 300\ 097\ln\dot{\varepsilon})T^*] \quad (14)$$

The comparison of flow stress-strain curves of measured and predicted data by the M-J-C model at different strain rates is shown in Fig.11.

2.3 Modified Z-A model

In contrast, the Zerilli-Armstrong (Z-A) model has different expressions for different crystal structures. It is suited for body-centered cube (bcc) and face-centered cube (fcc) metals. The crystal structure of C71500 alloy is fcc and the expression is as follows[18]:

Table 2 Fitting parameters for the M-J-C model

A_1	B_1	B_2	C_1	λ_1	λ_2
136.8453	293.9874	−279.723	0.073 09	−0.003	0.000 300 097

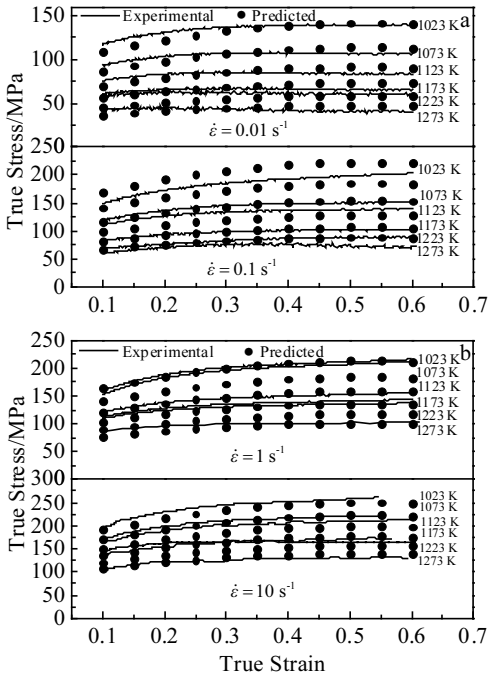

Fig.11 Comparison of flow stress of measured and predicted data by the M-J-C model: (a) 0.01 s^{-1} and 0.1 s^{-1}; (b) 1 s^{-1} and 10 s^{-1}

$$\sigma=A_0+A_1\varepsilon^n\exp(-A_2T+A_3T\ln\dot{\varepsilon}) \quad (15)$$

where σ, ε, $\dot{\varepsilon}$ and T are the same meaning as those in Eq.(1); A_0 is the thermal component of yield stress; A_1, A_2, A_3 and n are the material parameters.

The modified Z-A model for predicting high temperature flow behavior of material can be represented as follows[19]:

$$\sigma=(C_1+C_2\varepsilon^n)\exp[-(C_3+C_4\varepsilon)T^*+(C_5+C_6T^*)\ln\dot{\varepsilon}^*] \quad (16)$$

where $\dot{\varepsilon}^*=\dot{\varepsilon}/\dot{\varepsilon}_0$ is the dimensionless strain rate with $\dot{\varepsilon}$ being the strain rate and $\dot{\varepsilon}_0$ being the reference strain rate, respectively; $T^*=T-T_r$, T and T_r are the current and reference temperatures, respectively; C_1, C_2, C_3, C_4, C_5, C_6 and n are material constants.

The reference temperature and strain rate are just the same as the previous model. According to Eq.(16), material constants can be gained when $\dot{\varepsilon}^*=1$.

$$\sigma=(C_1+C_2\varepsilon^n)\exp[-(C_3+C_4\varepsilon)T^*] \quad (17)$$

Take natural logarithm on both sides of Eq.(17):

$$\ln\sigma=\ln(C_1+C_2\varepsilon^n)-(C_3+C_4\varepsilon)T^* \quad (18)$$

By substituting the obtained experimental flow stress data into Eq.(18), the relationship between $\ln\sigma$ and T^* is shown in Fig.12. The values of $\ln(C_1+C_2\varepsilon^n)$ and $-(C_3+C_4\varepsilon)$ can be gained from the intercept I_1=5.417 47 and the slope S_1=−0.002 91, respectively. Therefore,

$$I_1=\ln(C_1+C_2\varepsilon^n) \quad (19)$$

Eq.(19) can be derived:

$$\ln(\exp I_1-C_1)=\ln C_2+n\ln\varepsilon \quad (20)$$

where C_1 is the yield stress at T=1023 K and $\dot{\varepsilon}^*=1$. By substituting C_1 into Eq.(20), C_2=5.0753 and n=0.349 68 can be calculated from the intercept and slope of the relationship between $\ln(\exp I_1-C_1)$ and $\ln\varepsilon$ shown in Fig.13.

Similarly, the slope represented by Eq.(18) can be written as:

$$S_1=-(C_3+C_4\varepsilon) \quad (21)$$

The relationship between S_1 and ε is shown in Fig.14. Therefore, from Fig.14, $-C_3$, and $-C_4$ can be obtained as the intercept and slope, respectively.

Take natural logarithm on both sides of Eq.(16):

$$\ln\sigma=\ln(C_1+C_2\varepsilon^n)-(C_3+C_4\varepsilon)T^*+(C_5+C_6T^*)\ln\dot{\varepsilon}^* \quad (22)$$

The $\ln\sigma$ and $\ln\dot{\varepsilon}^*$ plot gives the value of $C_5+C_6T^*$ as the slope

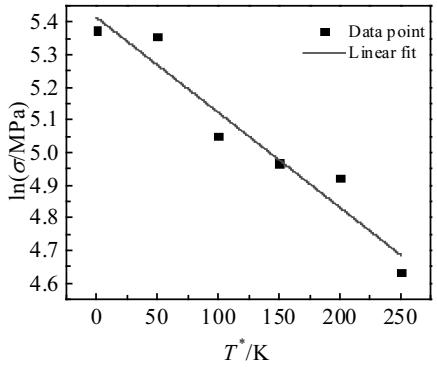

Fig.12 Relationship between $\ln\sigma$ and T^* at reference strain rate of 0.2

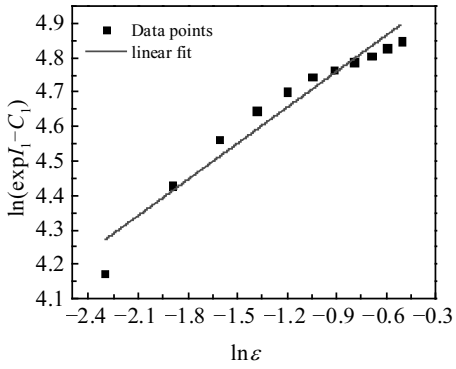

Fig.13 Relationship between $\ln(\exp I_1-C_1)$ and $\ln\varepsilon$ for Z-A model

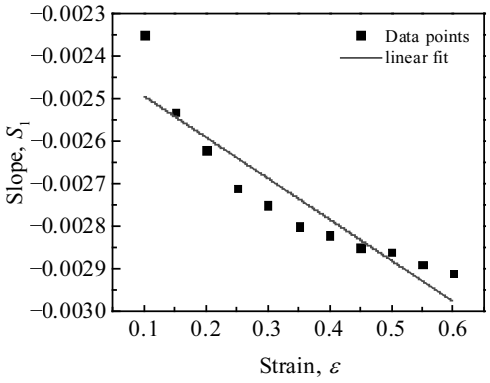

Fig.14 Relationship between S_1 and ε

S_2 shown in Fig.15. For different temperatures, the slope S_2 can be represented as follows:

$$S_2=C_5+C_6T^* \quad (23)$$

C_5=0.084 46 and C_6=0.000 300 125 can be calculated from the relationship between S_2 and T^* in Fig.16. The material constants for the modified Z-A model are listed in Table 3.

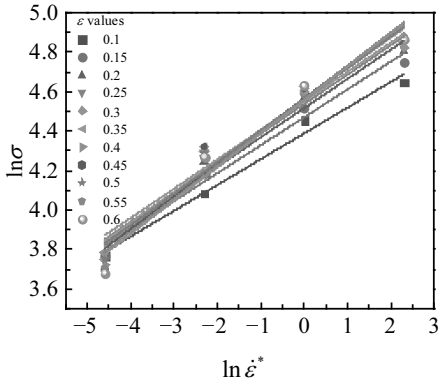

Fig.15 Relationship between $\ln\sigma$ and $\ln\dot{\varepsilon}^*$

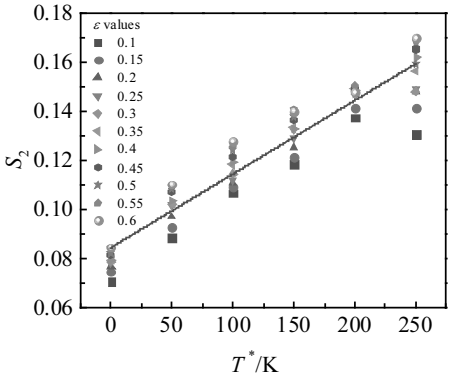

Fig.16 Relationship between S_2 and T^*

Then the specific constitutive equation based on modified Z-A model is:

$$\sigma=(97.069\,55+160.020\,19\varepsilon^{0.349\,68})\exp[-(0.0024+0.000\,965\,455\varepsilon)T^* +(0.084\,46+0.000\,300\,125T^*)\ln\dot{\varepsilon}^*] \quad (24)$$

The comparison of flow stress-strain curves of measured and predicted data by the modified Z-A model is shown in Fig.17.

2.4 Constitutive Arrhenius-type model

Arrhenius-type equation[20,21] is widely used in high temperature deformation, which includes the relationship among strain rate, forming temperature and flow stress:

$$Z=\dot{\varepsilon}\exp\left(\frac{Q}{RT}\right) \quad (25)$$

$$Z=AF(\sigma) \quad (26)$$

where

$$F(\sigma)=\begin{cases}\sigma^{n_1}, & \alpha\sigma<0.8\\ \exp(\beta\sigma), & \alpha\sigma>1.2\\ [\sinh(\alpha\sigma)]^n, & \text{for all } \alpha\sigma\end{cases} \quad (27)$$

Table 3 Parameters for the modified Z-A model

C_1	C_2	C_3	C_4	C_5	C_6	n
97.069 55	160.020 19	0.0024	0.000 965 455	0.084 46	0.000 300 125	0.349 68

$$\dot{\varepsilon}=\begin{cases}A_1\sigma^{n_1}\exp\left(-\dfrac{Q}{RT}\right), & \alpha\sigma<0.8\\ A_2\exp(\beta\sigma)\exp\left(-\dfrac{Q}{RT}\right), & \alpha\sigma>1.2\\ A[\sinh(\alpha\sigma)]^n\exp\left(-\dfrac{Q}{RT}\right), & \text{for all } \alpha\sigma\end{cases} \quad (28)$$

where $\dot{\varepsilon}$, R, T, Q and σ is the strain rate (s^{-1}), gas constant (8.314 J/(mol·K)), absolute temperature (K), activation energy of hot deformation (kJ/mol) and characteristic stress (MPa), respectively; A, α, β, n and n_1 are all the material constants, $\alpha=\beta/n_1$[22], and A_1 and A_2 are related to temperatures.

Power law and exponential law can be used at low stress level ($\alpha\sigma<0.8$) and high stress level ($\alpha\sigma>1.2$), and hyperbolic sine law can be applied to the whole stress range.

Take the logarithm of both sides of Eq.(28), the following formula can be obtained:

$$\ln\dot{\varepsilon}=\ln A_1+n_1\ln\sigma+\left(-\frac{Q}{RT}\right) \quad (29)$$

$$\ln\dot{\varepsilon}=\ln A_2+\beta\sigma+\left(-\frac{Q}{RT}\right) \quad (30)$$

$$\ln\dot{\varepsilon}=\ln A+n\ln[\sinh(\alpha\sigma)]+\left(-\frac{Q}{RT}\right) \quad (31)$$

The values of material constant n_1=6.794 147 and β=0.0552 MPa^{-1} can be obtained from the average slope of the line using linear regression method in Fig.18a and 18b. Therefore the value of $\alpha=\beta/n_1$=0.008 125 MPa^{-1}.

From the linear curve of $\ln\dot{\varepsilon}$-$\ln[\sinh(\alpha\sigma)]$ at different temperatures, n=5.732 93 can be fitted by the average slope of

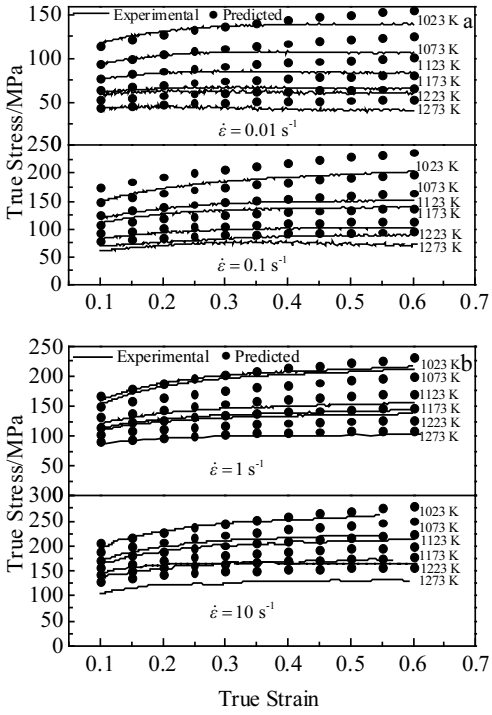

Fig.17 Comparison of flow stress between measured and predicted data by modified Z-A model: (a) 0.01 s^{-1} and 0.1 s^{-1}; (b) 1 s^{-1} and 10 s^{-1}

linear regression analysis, as shown in Fig.18c.

$$n=\left\{\frac{\partial\ln\dot{\varepsilon}}{\partial\ln[\sinh(\alpha\sigma)]}\right\}_T \quad (32)$$

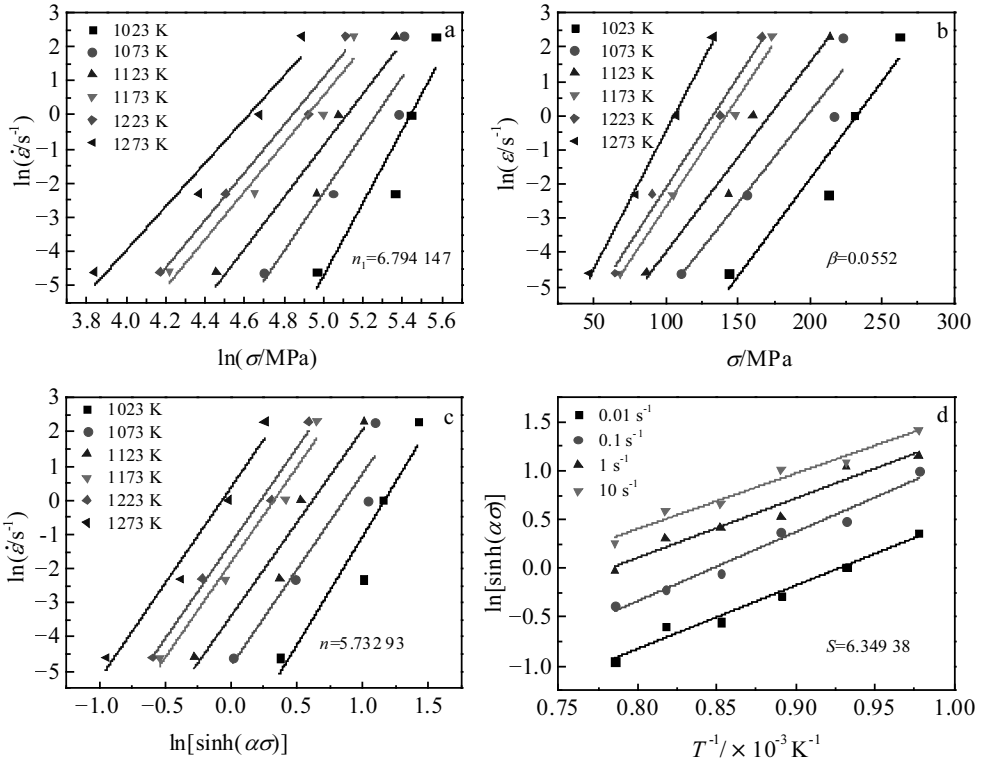

Fig.18 Relationship of $\ln\dot{\varepsilon}$-$\ln\sigma$ (a), $\ln\dot{\varepsilon}$-σ (b), $\ln\dot{\varepsilon}$-$\ln[\sinh(\alpha\sigma)]$ (c), and $\ln[\sinh(\alpha\sigma)]$-$1/T$ (d)

S is the mean slope of plots of $\ln[\sinh(\alpha\sigma)]$-$1/T$ at various strain rates, which equals 6.349 38, as shown in Fig.18d.

$$S=\left\{\frac{\partial\ln[\sinh(\alpha\sigma)]}{\partial(1/T)}\right\}_{\dot{\varepsilon}} \tag{33}$$

Given the strain rate, activation energy Q can be expressed as:

$$Q=RnS \tag{34}$$

The calculated average value of Q is 300.4839 kJ/mol. In addition, A=2.900 25×10^{12} s^{-1} can be easily obtained from linear fitting of $\ln[\sinh(\alpha\sigma)]$-$\ln Z$ with substituting previously estimated Q into Eq.(28), as shown is Fig.19.

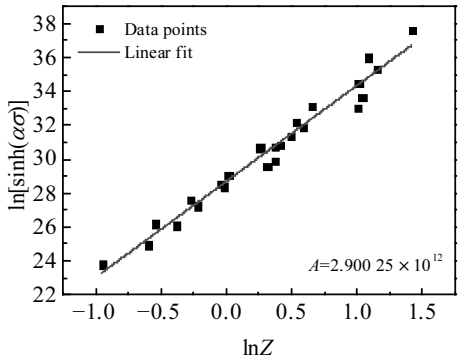

Fig.19 Relationship between $\ln[\sinh(\alpha\sigma)]$-$\ln Z$

In Eq.(28), it is considered that the influence of strain on high-temperature flow behavior is not significant, so it can be ignored. However, related studies have shown that in the entire strain range, strain has significant influence on the material constants (i.e. α, n, Q and ln$A$), as illustrated in Fig.20. In ZHMn34-2-2 manganese brass[41], BFe10-1-2 alloy[36], AZ61Mg alloy[42], α-Ti alloy[27] and Cu-Zr-Ce alloy[31,43], the similar strain effect was observed. Therefore, the flow stress can be predicted more accurately after considering the strain compensation.

Strain compensation is widely used for improving the prediction accuracy[19,44,45]. The polynomial function is applied to fit the material constants, and the fitting accuracy is determined according to the correlation and accuracy. The fifth order polynomial has good correlation and generalization, as shown in Eq.(35). And the coefficient values of polynomial function are listed in Table 4.

$$\begin{cases}\alpha=\alpha_0+\alpha_1\varepsilon+\alpha_2\varepsilon^2+\alpha_3\varepsilon^3+\alpha_4\varepsilon^4+\alpha_5\varepsilon^5\\ n=n_0+n_1\varepsilon+n_2\varepsilon^2+n_3\varepsilon^3+n_4\varepsilon^4+n_5\varepsilon^5\\ Q=Q_0+Q_1\varepsilon+Q_2\varepsilon^2+Q_3\varepsilon^3+Q_4\varepsilon^4+Q_5\varepsilon^5\\ \ln A=A_0+A_1\varepsilon+A_2\varepsilon^2+A_3\varepsilon^3+A_4\varepsilon^4+A_5\varepsilon^5\end{cases} \tag{35}$$

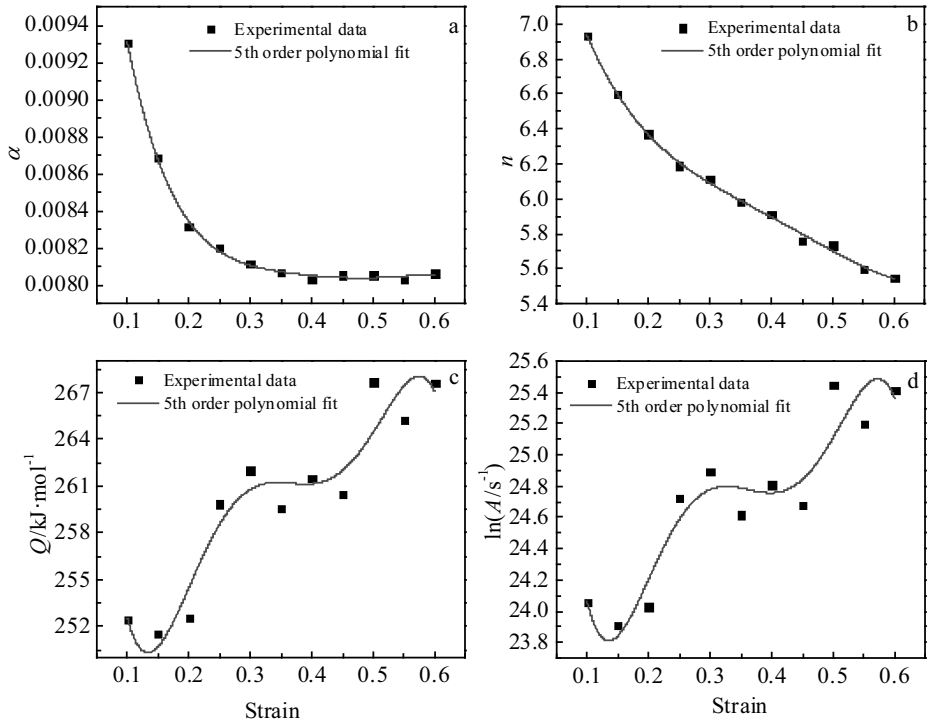

Fig.20 Variation of material constants α (a), n (b), Q (c), and ln$A$ (d) with strain

Table 4 Polynomial coefficients of the fitted material constants α, n, Q and ln$A$ for constitutive Arrhenius-type model

α	n	Q	ln$A$
α_0=0.012 25	n_0=8.112 13	Q_0=315.872 38	A_0=30.825 67
α_1=−0.045 69	n_1=−16.175 69	Q_1=−1352.8236	A_1=−144.366 62
α_2=0.204 35	n_2=51.790 23	Q_2=9951.515 23	A_2=1063.740 14
α_3=−0.463 03	n_3=−81.972 98	Q_3=−32 045.921 07	A_3=−3452.885 04
α_4=0.524 68	n_4=46.516 22	Q_4=47 447.110 28	A_4=5155.241 18
α_5=−0.235 67	n_5=2.182 05	Q_5=−26 323.2364	A_5=−2881.811 94

From Eq.(25) and (28), the constitutive equations of related materials can be obtained as follows:

$$\sigma=\frac{1}{\alpha(\varepsilon)}\ln\left\{\left(\frac{Z}{A(\varepsilon)}\right)^{1/n(\varepsilon)}+\left[\left(\frac{Z}{A(\varepsilon)}\right)^{2/n(\varepsilon)}+1\right]^{1/2}\right\} \quad (36)$$

The comparison of flow stress-strain curves of experimental and predicted data by the constitutive Arrhenius-type model is shown in Fig.21.

2.5 Modified F-B-Z model

The flow stress value predicted by Fields-Backofen-Zhang (F-B-Z) model at high strain rate shows the disadvantage of large deviation. Lin et al[27] added the strain rate term (u) to this model, which is called the modified F-B-Z model, as shown in Eq.(37):

$$\sigma=K\varepsilon^{n}\dot{\varepsilon}^{m}\exp(bT+s\varepsilon+u\dot{\varepsilon}) \quad (37)$$

where K, n and m are the strength, strain hardening and strain rate sensitivity exponent, respectively; s is softening item; b is temperature item.

Assuming that the relationship between flow stress and true strain in plastic deformation stage satisfies Eq.(37), then Eq.(37) can be expressed as

$$\ln\sigma=\ln K+n\ln\varepsilon+m\ln\dot{\varepsilon}+bT+s\varepsilon+u\dot{\varepsilon} \quad (38)$$

Multivariate linear regression analysis is performed to obtain the parameters in Eq.(38). The material constants of the modified F-B-Z model are listed in Table 5.

Then the constitutive equation based on modified F-B-Z model can be obtained as follows:

$$\sigma=6661.061\varepsilon^{0.247\ 53}\dot{\varepsilon}^{0.122\ 25}\times \exp(-0.002\ 94T-0.414\ 57\varepsilon-0.011\ 52\dot{\varepsilon}) \quad (39)$$

The comparison of flow stress-strain curves of experimental and predicted data by modified F-B-Z model is shown in Fig.22.

2.6 Zhou-Guan model

Zhou-Guan (Z-G) model[28] is widely used to express the

Table 5 Parameters of the modified F-B-Z model for the prediction of the high temperature flow stress of C71500 alloy

K	n	m	b	s	u
6661.061	0.247 53	0.122 25	−0.002 94	−0.414 57	−0.011 52

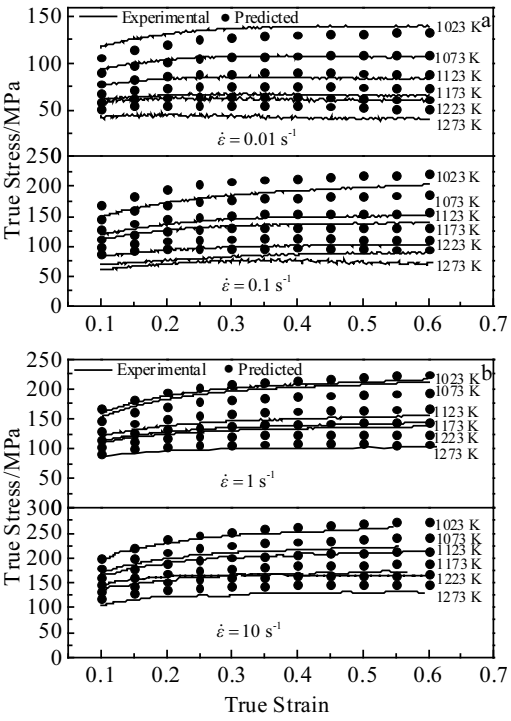

Fig.21 Experimental and predicted flow stress by strain compensated Arrhenius-type equation at different strain rates: (a) 0.01 s^{-1} and 0.1 s^{-1}; (b) 1 s^{-1} and 10 s^{-1}

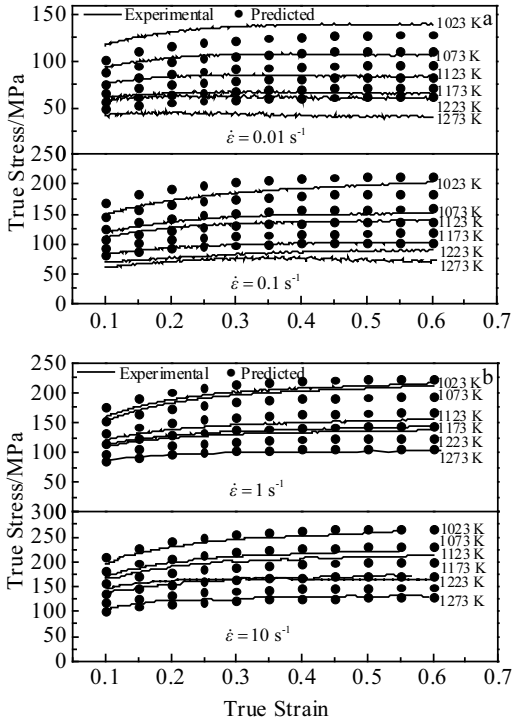

Fig.22 Experimental and predicted flow stress by modified F-B-Z model at different strain rates: (a) 0.01 s^{-1} and 0.1 s^{-1}; (b) 1 s^{-1} and 10 s^{-1}

relationships among the strain rate, forming temperature and flow stress, especially for steel:

$$\sigma=\sigma_0 X_T X_{\dot{\varepsilon}} X_{\varepsilon} \tag{40}$$

with:

$$X_T=\mathrm{e}^{a_1+a_2 T}$$

$$X_{\dot{\varepsilon}}=\left(\frac{\dot{\varepsilon}}{10}\right)^{a_3 T+a_4}$$

$$X_{\varepsilon}=a_6\left(\frac{\varepsilon}{0.4}\right)^{a_5}-(a_6-1)\left(\frac{\varepsilon}{0.4}\right)$$

$$T=\frac{t+273}{1000}$$

where σ_0 is the datum deformation resistance, i.e., deformation resistance at 1023 K, ε=0.02 and $\dot{\varepsilon}=1\ s^{-1}$, which equals to 165.75 MPa; t is the deformation temperature (°C); a_1~a_6 are material parameters.

The stress-strain curve data obtained from the experiment are brought into the model, and the data are regressed by Origin 9 software. The regression coefficients of the model are shown in Table 6.

Then the specific constitutive equation based on Z-G model can be obtained as follows:

$$\sigma=165.75\mathrm{e}^{-2.331\ 57T+2.550\ 14}\times\left(\frac{\dot{\varepsilon}}{10}\right)^{0.286\ 79T-0.214\ 81}\times\left[1.244\ 25\left(\frac{\varepsilon}{0.4}\right)^{0.262\ 11}-1.244\ 25\left(\frac{\varepsilon}{0.4}\right)\right] \tag{41}$$

Table 6 Parameters of the Z-G model for predicting high temperature flow stress of C71500 alloy

σ_0	a_1	a_2	a_3	a_4	a_5	a_6
165.75	−2.331 57	2.550 14	0.286 79	−0.214 81	0.262 11	1.244 25

The comparison of flow stress-strain curves of experimental and predicted data by the Z-G model is shown in Fig.23.

3 Discussion

Correlation coefficient (R), root mean square error (RMSE) and average absolute relative error (AARE) are introduced to verify the prediction effectiveness of the mentioned constitutive equations:

$$R=\frac{\sum_{i=1}^{N}(E_i-\bar{E})(P_i-\bar{P})}{\sum_{i=1}^{N}(E_i-\bar{E})^2(P_i-\bar{P})^2} \tag{42}$$

$$\mathrm{RMSE}=\sqrt{\frac{1}{N}\sum_{i=1}^{N}(E_i-P_i)^2} \tag{43}$$

$$\mathrm{AARE}(\%)=\frac{1}{N}\sum_{i=1}^{N}\left|\frac{(E_i-P_i)}{E_i}\right|\times 100\% \tag{44}$$

where E and P are the experimental flow stress and the predicted value; $\bar{E}$ and $\bar{P}$ are the mean values of E and P; N is the total number of result obtained from the experiment.

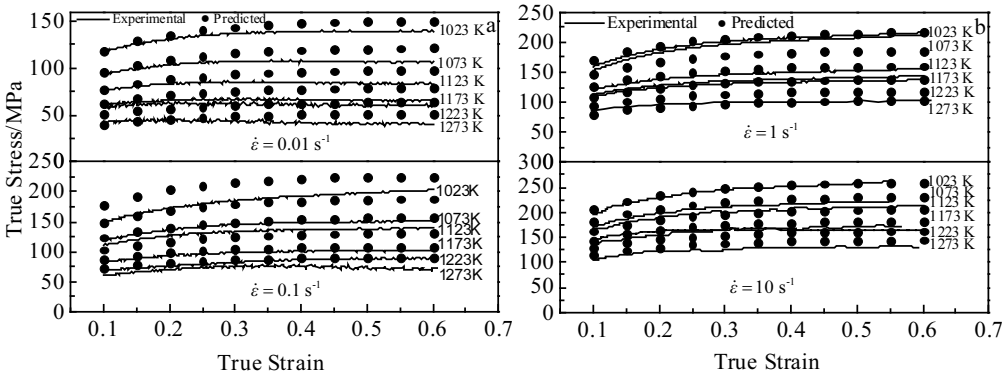

Fig.23 Experimental and predicted flow stress by strain compensated Z-G model at different strain rates: (a) 0.01 s^{-1} and 0.1 s^{-1}; (b) 1 s^{-1} and 10 s^{-1}

The correlation coefficient represents the strength of the linear relationship between the measured and the calculated values. However, a higher *R* value may not necessarily indicate a better fitting relationship, because the variation trend of the equation may have deviation. RMSE and AARE are calculated by comparing the relative errors one by one. Smaller the values of RMSE and AARE, better the predictability of the representative equation. The *R*, RMSE and AARE values under different constitutive models are listed in Table 7.

It can be seen from Table 7 that the *R* values of other models are above 0.98 except for J-C and Z-A models, which indicates that the M-J-C, Arrhenius-type, F-B-Z and Z-G models can well describe the linear trend of C71500 alloy, and Z-G model shows better correlation considering RMSE and AARE. From the correlation of M-J-C and Z-G models in Fig.24b and 24f, it can be seen that the fitting results of M-J-C model are more accurate at low strain rate, but when the strain rate reaches 10 s^{-1}, the calculated results of Z-G model are much different from the actual ones, and the calculated results of Z-G model are better than those of the M-J-C model at higher strain rate. Considering the number of parameters of the model, it is relatively easy to calculate the parameters of other models except Arrhenius-type model with 5~7 parameters. Therefore, the Z-G model is more accurate and faster for predicting the flow stress of C71500 alloy.

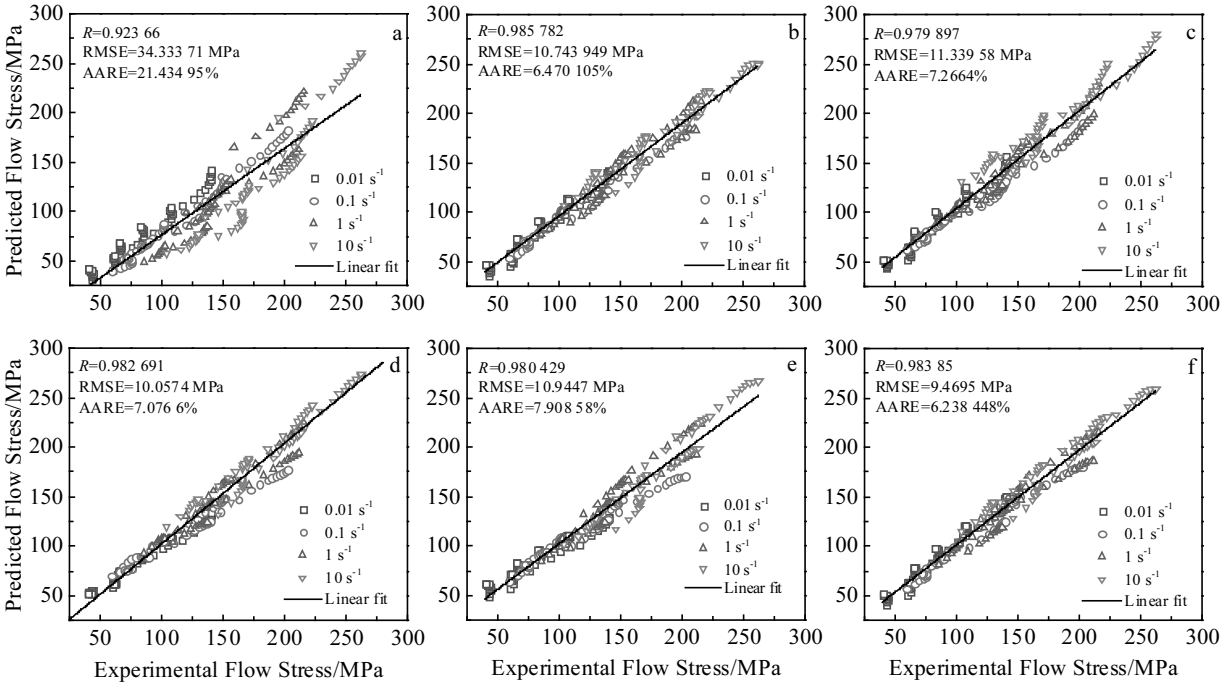

Fig.24 Correlation between the experimental and predicted flow stress values by J-C model (a), M-J-C model (b), Z-A model (c), Arrhenius-type model (d), F-B-Z model (e), and Z-G model (f)

Table 7 *R*, RMSE and AARE values under different constitutive models

Parameter	J-C	M-J-C	Z-A	Arrhenius	F-B-Z	Z-G
R	0.923 66	0.985 78	0.979 90	0.982 69	0.980 43	0.983 85
RMSE/MPa	34.333 71	10.743 95	11.339 58	10.057 42	10.944 74	9.469 51
AARE/%	21.434 95	6.470 11	7.266 43	7.076 61	7.908 58	6.238 45

4 Conclusions

1) The fitting results of the thermal deformation behavior of C71500 alloy in the temperature range of 1023~1273 K and the strain rate range of 0.01~10 s^{-1} through Johnson-Cook, modified Johnson-Cook, modified Zerilli-Armstrong, Arrhenius-type, Fields-Backofen-Zhang and Zhou-Guan models are obtained. The six models can well describe the linear trend of C71500 alloy.

2) Using correlation coefficient (*R*), root mean square error (RMSE) and average absolute relative error (AARE) to verify the predictive effectiveness of different constitutive equations, the results show that Z-G model has a better correlation.

3) Zhou-Guan model has better prediction performance for deformation resistance of C71500 alloy at various strain rates and temperatures according to the fitting results, the number of model parameters and the fitting operation time.

References

1 Cincera S, Barella S, Bellogini M. *Journal of Failure Analysis and Prevention*[J], 2012, 12(3): 300

2 Ezuber H M. *Anti-Corrosion Methods and Materials*[J], 2009, 56(3): 168

3 Zhang Jie, Wang Qing, Wang Yingmin *et al*. *Journal of Alloys and Compounds*[J], 2010, 505(2): 505

4 Beccaria A M, Crousier J. *British Corrosion Journal*[J], 2013, 26(3): 215

5 Bautista B E T, Carvalho M L, Seyeux A *et al*. *Bioelectrochemistry*[J], 2014, 97: 34

6 Bhattacharya S, Dinda G P, Dasgupta A K *et al*. *Journal of Materials Science*[J], 2014, 49(6): 2415

7 Yan Binjiang, Xian Gailiu, Xiao Junzhang *et al*. *Chinese Journal of Nonferrous Metals*[J], 2014, 24(9): 2322

8 Drolenga L J P, Ijsseling F P, Kolster B H. *Materials and Corrosion*[J], 1983, 34(4): 167

9 Bautista B E T, Wikieł A J, Datsenko I *et al*. *Journal of Electroanalytical Chemistry*[J], 2015, 737: 184

10 Wei Mumeng, Yang Bojun, Liu Yangyang *et al*. *Journal of Chinese Society for Corrosion and Protection*[J], 2016, 36(6): 513

11 Mao Xiangyang, Feng Fang, Jiang Jianqing *et al*. *Rare Metals*[J], 2009, 28(6): 590

12 Mao Xiangyang, Fang Feng, Yang Fan *et al*. *Journal of Materials Processing Technology*[J], 2009, 209(4): 2145

13 Gu Caixiang, Zhang Xiaolei, Zhao Xiangbo. *Ship Engineering*[J], 2014(3): 10 (in Chinese)

14 Lin Y C, Chen M S, Zhong J. *Computational Materials Science*[J], 2008, 42(3): 470

15 Hajari A, Morakabati M, Abbasi S M *et al*. *Materials Science and Engineering A*[J], 2016, 681: 103

16 Johnson G R, Cook W H. *Proceedings of the 7th International Symposium on Ballistics*[J], 1983, 21(1): 541

17 Chen X M, Lin Y C, Liu G. *Materials Science and Engineering A*[J], 2010, 527(26): 6980

18 Zerilli F J, Armstrong R W. *Journal of Applied Physics*[J], 1987, 61(5): 1816

19 Samantaray D, Mandal S, Borah U *et al*. *Materials Science and Engineering A*[J], 2009, 526(1-2): 1

20 Sellars C M, McTegart W J. *Acta Metallurgica*[J], 1966, 14(9): 1136

21 Jonas J J, Sellars C M, Tegart W J M G. *Metallurgical Reviews*[J], 1969, 14(1): 1

22 Wang Zhenjun, Qi Lehua, Zhou Jiming *et al*. *Computational Materials Science*[J], 2011, 50(8): 2422

23 Fields D S, Bachofen W A. *Proceeding of American Society for Testing and Materials*[J], 1957, 57: 1259

24 Zhou M, Lin Y C, Deng J *et al*. *Materials & Design*[J], 2014, 59(6): 141

25 Jia Weitao, Xu Shuang, Le Qichi *et al*. *Materials & Design*[J], 2016, 106: 120

26 Lin Peng, He Zhubin, Shijian Yuan *et al*. *Materials Science and Engineering A*[J], 2012, 556(11): 617

27 Lin Yanli, Zhang Kun, He Zhubin *et al*. *Journal of Materials Engineering and Performance*[J], 2018, 27(5): 1

28 Guan Kezhi, Zhou Jihua, Zhu Qisheng *et al*. *Journal of Beijing Iron and Steel Institute*[J], 1983(1): 123

29 Huang S, Khan A S. *Experimental Mechanics*[J], 1991, 31(2): 122

30 Kumar S, Aashranth B, Davinci M A *et al*. *Journal of Materials Engineering and Performance*[J], 2018, 27(4): 2024

31 Zhao Xinhai, Liu Dandan, Wu Xianghong *et al*. *Journal of Central South University*[J], 2018, 25(5): 1013

32 Gao Jun, Li Miaoquan, Liu Shaofei *et al*. *Rare Metals*[J], 2017, 36(2): 1

33 Mo Yongda, Jiang Yanbin, Liu Xinhua *et al*. *Journal of Materials Processing Technology*[J], 2016, 235: 75

34 Zhou Zhaohui, Fan Qichao, Xia Zhihui *et al*. *Journal of Materials Science and Technology*[J], 2017, 33(7): 637

35 Cai Jun, Wang Kuaishe, Wang Wen. *Rare Metal Materials and Engineering*[J], 2016, 45(10): 2549

36 Cai Jun, Wang Kuaishe, Miao Chengpeng *et al*. *Materials &*

Design[J], 2015, 65: 272
37 Cai Jun, Wang Kuaishe, Peng Zhai *et al*. *Journal of Materials Engineering and Performance*[J], 2015, 24(1): 32
38 Qiang Tanjin, Zhan Mei, Liu Shuai *et al*. *Materials Science and Engineering A*[J], 2015, 631(1): 214
39 Li Hongbin, Zheng Mingyue, Tian Wei *et al*. *Material for Mechanical Engineering*[J], 2016, 40(11): 31
40 Cheng Yongqi, Zhang Hui, Chen Zhenhua *et al*. *Journal of Materials Processing Technology*[J], 2008, 208(1-3): 29
41 Wang Menghan, Wei Kang, Li Xiaojuan *et al*. *Journal of Central South University*[J], 2018, 25(7): 1560
42 Liao C H, Wu H Y, Lee S *et al*. *Materials Science and Engineering A*[J], 2013, 565(10): 1
43 Zhang Y, Sun H, Volinsky A A *et al*. *Journal of Materials Engineering and Performance*[J], 2018, 27(2): 728
44 Mandal S, Rakesh V, Sivaprasad P V *et al*. *Materials Science and Engineering A*[J], 2009, 500(1-2): 114
45 Li Jiang, Li Fuguo, Cai Jun *et al*. *Computational Materials Science*[J], 2013, 71: 56

不同本构方程对 C71500 白铜合金热压缩的拟合分析

高　鑫[1,2,3]，武会宾[4]，唐　狄[1]，李德富[2]，刘　明[5]，周向东[3]

(1. 北京科技大学 工程技术研究院，北京 100083)

(2. 北京有色金属研究总院，北京 100088)

(3. 无锡隆达金属材料有限公司，江苏 无锡 214105)

(4. 北京科技大学 钢铁共性协同创新中心，北京 100083)

(5. 西安交通大学 机械结构强度与振动国家重点实验室，陕西 西安 710049)

摘　要：在 Gleeble-3500 热模拟机上，获得了 C71500 白铜合金在 1073~1273 K 温度范围和 0.01~10 s^{-1} 应变速率范围下等温压缩试验的真实应力应变数据。采用 Johnson-Cook、改良 Johnson-Cook、Zerilli-Armstrong、Arrhenius、Fields-Backofen-Zhang 和 Zhou-Guan 模型对高温流动应力本构方程进行了回归分析。通过比较精度、相关系数（*R*）、均方根误差（RMSE）、平均绝对相对误差（AARE）、不确定度和计算时间，评价了 6 种模型的适用性。根据参数和时间消耗的拟合结果，Zhou-Guan (Z-G)模型是预测 C71500 合金在不同应变率和温度下变形抗力的最佳模型。建立了 C71500 合金最合适的热变形本构方程，为该合金热加工工艺设计和热变形过程模拟分析提供了基础数据。另外，该研究方法可以为同一领域的研究提供重要的参考。

关键词：白铜；本构方程；热变形；流动应力

作者简介：高　鑫，男，1984 年生，博士生，高级工程师，北京科技大学工程技术研究院，北京 100083，E-mail: 15901462422@163.com